



A voyage planning tool for ships sailing between Europe and Asia via the Arctic

Downloaded from: <https://research.chalmers.se>, 2023-05-05 01:37 UTC

Citation for the original published paper (version of record):

Li, Z., Ringsberg, J., Rita, F. (2021). A voyage planning tool for ships sailing between Europe and Asia via the Arctic. *Ships and Offshore Structures*, 15(S1): S10-S19.
<http://dx.doi.org/10.1080/17445302.2020.1739369>

N.B. When citing this work, cite the original published paper.



A voyage planning tool for ships sailing between Europe and Asia via the Arctic

Zhiyuan Li , Jonas W. Ringsberg & Francisco Rita

To cite this article: Zhiyuan Li , Jonas W. Ringsberg & Francisco Rita (2021) A voyage planning tool for ships sailing between Europe and Asia via the Arctic, Ships and Offshore Structures, 15:sup1, S10-S19, DOI: [10.1080/17445302.2020.1739369](https://doi.org/10.1080/17445302.2020.1739369)

To link to this article: <https://doi.org/10.1080/17445302.2020.1739369>



© 2020 The Author(s). Published by Informa UK Limited, trading as Taylor & Francis Group



Published online: 11 Mar 2020.



Submit your article to this journal [↗](#)



Article views: 1477



View related articles [↗](#)



View Crossmark data [↗](#)



Citing articles: 2 View citing articles [↗](#)

A voyage planning tool for ships sailing between Europe and Asia via the Arctic

Zhiyuan Li , Jonas W. Ringsberg  and Francisco Rita

Department of Mechanics and Maritime Sciences, Chalmers University of Technology, Gothenburg, Sweden

ABSTRACT

The Arctic is rapidly transforming into a navigable ocean because of global warming. Consequently, a large percentage of the sailing distance between Europe and Asia could be saved by alternatively sailing through the Arctic. However, taking Arctic routes is fraught with risks and additional costs due to sea ice. The major purpose of this study is to improve safety and fuel efficiency of Arctic ships, which is achieved by voyage optimization upon frequently updated meteorological, oceanographic and ice forecasting. The resistance model accounts for both ice thickness and ice concentration of unconsolidated Arctic sea ice in summer. Ice-induced risks defined in the Polar Operational Limit Assessment Risk Indexing System (POLARIS) are dealt as constraint. Other constraints such as avoidance of land and shallow water are also included. These functions are demonstrated by the two case study vessels sailing between Rotterdam and Shanghai via both the Arctic and the traditional routes.

ARTICLE HISTORY

Received 8 December 2019
Accepted 3 March 2020

KEYWORDS

Arctic transit; bathymetry in the Arctic; ice resistance; Polar Operational Limit Assessment Risk Indexing System (POLARIS); voyage planning

1. Introduction

The Arctic is transforming into a navigable ocean because of global warming. On 1st July 1991, the Russian Federation opened up the Northern Sea Route (NSR) for foreign traffic and thereby opened a new sea route between Europe and Asia (Ostreng et al. 2013). Substantial reductions in voyage times and fuel consumption can be achieved using the NSR compared to the Suez Canal Route (SCR) and the route around South Africa. For instance, in 2013, a general cargo ship, MV COSCO Yongsheng departed from Taicang in China on 15th August and sailed via the NSR instead of the traditional route via the Malacca Strait and the Suez Canal. She arrived at Rotterdam in the Netherlands on 10th September, reducing the voyage distance by 2800 nautical miles and the sailing time by 9 days (COSCO 2017).

The MV COSCO Yongsheng's case, however, needs to be reckoned as an ideal case. The vessel spent 7.4 days on the NSR at an average speed of 14.1 knots, very close to her service speed of 14.8 knots. This smooth passage of the NSR depends on the following facts: firstly, ice conditions along the NSR are in general mild in late August and early September. The most severe ice MV Cosco Yongsheng encountered was a combination of 4/10th of medium first-year ice (70–120 cm) and 5/10th of thin first-year second stage ice (50–70 cm), close to the Vilkitsky Strait. Secondly, MV Cosco Yongsheng was escorted by the Russian nuclear-powered icebreaker IB 50 Let Pobedy for 127 h, covering a major percentage of the voyage in the NSR waters (Zhang et al. 2017).

Shipping via the Arctic is always associated with additional costs as well as risks due to the remoteness and the special environmental conditions in Arctic areas. Ice in Arctic waters

not only induces additional resistance and thus increases fuel consumption but also may cause damage to the ship hull and propeller. Therefore, when sailing in Arctic waters, voluntary speed reductions are common practice. In addition, alternative routes must be taken under severe ice conditions, or when iceberg and large multi-year ice bits are expected along the planned route. This indicates the need of a voyage planning tool (VPT) for ships entering Arctic waters.

2. State of the art

2.1. Arctic ice condition

Despite the reduction in ice cover in the polar seas, Arctic waters are only navigable for commercial shipping for a limited period during the year. For the NSR, the summer season typically starts in June and ends in November, which is somewhat longer than the season for the Northwest Passage (Pharand 2007). Statistics show that July to October accounts for approximately 63% of the total NSR voyages in recent years (Balmasov 2018). However, it needs to be highlighted that the Arctic summer season is expected to be continuously extended due to climate change. Some climate models predict that the navigation window will double for both the NSR and the Northwest Passage by the middle of this century and by then the trans-Pole route will be viable (Khon et al. 2010). The Arctic transit scenarios investigated in this study are limited to the summer months.

The NSR lies in Arctic waters close to Russia's northern coastline, as part of the Northeast Passage. The summer ice along the NSR differs significantly from those in other cold regions like the Baltic Sea or the Great Lakes in North America

in winter. Taking winter Baltic, for example, the sea surface is typically covered by a consolidated layer of ice that is termed as level ice. Most commercial ships even though ice-strengthened, need the assistance of icebreakers to open channels to enable operation. Along the NSR in summer, in contrast, continuous ice sheets are unlikely to be encountered. Instead, the encountered sea regime is typically composed of fragmented ice floes. The floating ice pieces can be of different sizes, and the water surface is only partly covered by ice. [Figure 1](#) illustrates the common ice fields during the summer in the Arctic and winter in the Baltic.

Another feature of summer Arctic ice is that multi-year ice (MYI) may be included in an ice regime that is dominated by first-year ice (FYI). In winter in the Baltic and the Great Lakes, only FYI exists, and it disappears every year when the winter is over. MYI is sea ice that has survived at least one summer, and for this reason, MYI is generally thicker than FYI. Moreover, MYI contains much less brine and more air pockets, making it much stiffer. When colliding with ships, MYI is more likely to damage the hull and propeller, and thus ought to be avoided. MYI exists in the Arctic. Along the NSR, the interior seas such as the Laptev Sea and the East Siberian Sea receive significant ice transported from the central Arctic Ocean, including some MYI floes ([Østreng 2013](#)).

2.2. Bathymetry along the NSR

The sea depth is another key parameter to consider for navigation along the NSR. Due to heavier and more persistent ice at higher latitudes, deep-draft routes closer to the Arctic basin are open for much shorter periods in comparison with the shallower routes near the northern edge of the Russian archipelago. The continental shelves of the NSR seas are unusually broad and shallow. [Figure 2](#) illustrates the sea depth in the Arctic, where the Arctic bathymetry data were obtained from the International Bathymetry Carhart of the Arctic ocean (IBCAO). It is seen that quite large areas in the Laptev Sea and the East Siberian Sea are shallower than 25 meters (marked in yellow), water depth near the coastline is even shallower. For instance, the Dmitry Laptev Strait and the Sannikov Strait in the New Siberian Islands are as shallow as 6.7 and 13 meters,

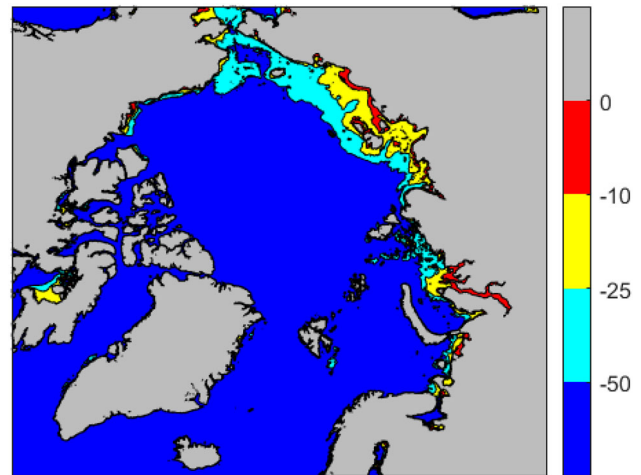


Figure 2. Water depth in the Arctic. (This figure is available in colour online.)

respectively ([Østreng 2013](#)). The bathymetry constraints along the NSR must be considered together with the ship draft when planning a voyage along the NSR.

2.3. Arctic voyage planning

Voyage planning for ships is currently supported by weather routing systems. Many environmental factors are considered in a weather routing system, such as waves, wind, current, and air and water temperatures. However, most existing weather routing systems are developed for open seas, which means sea ice and ice-induced resistance are not considered.

In recent years, several studies have discussed voyage planning in ice-covered waters. Kotovirta et al. (2009) presented a route optimisation system in ice-covered waters, making use of ship-borne Automatic Identification System (AIS) data. The proposed method was promoted for route optimisation in winter Baltic with level ice and ridged ice modelled. This method can however hardly be applied in Arctic transits due to the following facts: firstly, as mentioned previously, the Arctic ice scenarios in summer are different; secondly, the Arctic routes, especially along the NSR, are typically very



Figure 1. Examples of typical ice conditions in (left) summer Arctic (photo source: China COSCO Shipping Corporation), and in (right) winter Baltic (photo source: Swedish Maritime Administration). (This figure is available in colour online.)

remote from coastal AIS stations, which differs from the Baltic region.

Choi et al. (2010) presented Arctic transit analyses for icebreaking cargo vessels. Instead of lower ice-classed ships that enter the Arctic during the summer months, the target vessel types are those designed for year-around operations in the Arctic. Jeong et al. (2018) introduced a newly developed Arctic voyage planning system as well as the validation tests conducted onboard an Korean icebreaker in the East Siberian Sea. The presented main functions were promising, but the field trials were conducted mainly in higher latitude other than the normal Arctic shipping routes.

Researchers have investigated route optimisation algorithms in the Arctic. For example, Nam et al. (2013) introduced a simulation-based method to determine the optimal Arctic route using an advanced numerical sea ice model. The proposed model uses ice and environmental data by analyzing a numerical ice model which offers an analytical way to predict routes in coming years. The targeted ice type in this article is level/ridged ice. Choi et al. (2015) presented an uncertainty-based route planning model that can be applied in icy Arctic waters. In that paper, the path planning problem is solved by generating a map through the ensemble simulation of an ice model. And an uncertainty-based path planning model is proposed to find an optimal route under time-varying stochastic conditions. Zhang et al. (2018) proposed a method for planning Arctic sea routes under multiple-constraint conditions of physical and operational considerations. This article highlighted many important aspects for voyage planning for the Arctic route but detailed descriptions about the routing algorithm as well as the ice model are missing.

The above-mentioned studies provided valuable insights in voyage planning in the Arctic from various perspectives. However, a comprehensive voyage planning tool for Arctic transits meeting shipowners' needs on voyage planning in ice-infested waters has not been developed previously. In particular, the function for minimisation of fuel consumption is missing. In addition, most existing planning tools for Arctic operations target at ice-breaking vessels instead of commercial ships designed mainly for open water operations. Moreover, to the authors' knowledge, those tools are limited to Arctic operation, not for the entire voyage that is composed of both the Arctic leg and the open-water legs. For the latter, wave and wind are the major environmental factors to be considered. In such a context, this work develops a VPT that meets the shipowner's needs and demand by analyzing the entire journey and all boundary conditions. This is achieved by a single-objective optimisation for minimising the fuel consumption in various Arctic transit scenarios, with ice-induced risk index outcome (RIO), and avoidance of land and shallow water as the major constraints.

3. Ice resistance

The main objective of the VPT presented in this study is to find optimal routes regarding fuel consumption in sometimes ice-infested waters. It is thus crucial to include ice resistance in the ship energy performance model. Ice resistance can be

derived by numerical simulations based on first-principle approaches, but such simulations typically require longer computation time so hardly meet the requirement of real-time voyage planning. Thus, there is the need for a practical formula that predicts the ice resistance of a ship under various combinations of speeds and ice conditions.

Ice-induced resistance formulae have been investigated by many researchers. Jones (2004) made a comprehensive review on ship performance in ice. A majority of the models are supposed to estimate the force required to break level ice. Accordingly, the thickness of level ice or ridged ice is the only parameter considered. The commonly accepted ice resistance models of Riska et al. (1998), Enkvist (1972), and Lindquist (1989) are all in this category. A similar method was promoted by Juva and Riska (2002) to compute the resistance of brash ice in channel opened by icebreaker, in which the total thickness of accumulated brash ice in the middle of the channel is taken as the parameter. This approach is adopted in Finnish-Swedish Ice Class Rules (FSICR) for estimation of propulsion power of ice-classes vessel (TraFi 2010).

However, as mentioned in Section 2.1, ice conditions along the NSR in summer season differ obviously from those of the Baltic Sea in winter. Fragmented ice floes, instead of level ice or channel ice are most likely to be encountered by commercial ships. The ice resistance models mentioned in the previous paragraph are therefore unsuitable to be utilised in the VPT. Given the fact that the water is not fully covered by ice in summer Arctic, ice concentration should also be considered to evaluate ice resistance. Literature study reveals that few ice resistance models of fragmented ice floe have been proposed, while the major of such models were developed by Canadian researchers for the purpose of evaluating loads on moored offshore ships from drift ice. Spencer et al. (1992) proposed a method for ice resistance evaluation based on model tests. This method divides the total ice resistance into four independent components as shown in Equation (1): open water, ice buoyance, ice clear and ice breaking. All these components are scaled separately.

$$R_{\text{total}} = R_{\text{OW}} + R_B + R_C + R_{BR} \quad (1)$$

This model was further developed by Colbourne (2000). Due to the difficulty of moving an ice field in a model tank, the experiments were conducted by moving the model vessel with forward speed, which implies that the measured ice loads are in fact the ice resistance to the ship. In fragmented ice-floe fields, the ice-breaking component is very little and can be neglected. The component, R_{OW} , can be determined from corresponding open water model experiments. The remaining ice resistance force can thereby be determined from the total resistance force of ice model tests by subtracting the open water resistance. Colbourne's model introduced a so-called ice Froude number, Fr_p , which is composed of both ice thickness h_i and ice concentration C ; V is the ship speed, and g is the acceleration of gravity:

$$Fr_p = V / \sqrt{gh_i C} \quad (2)$$

Table 1. Prediction constants for various hull forms.

Prediction constants	Slender hull	Blunt hull
k_c	4.4	16.1
b	-0.8267	-1.7937
n	2	3

The ice resistance force, R_p , is calculated from the following formula:

$$R_p = 0.5C_P\rho_i B h_i V^2 C^n \quad (3)$$

where C_P is the ice force coefficient. B and ρ_i are the ship beam and the ice density, respectively. Mean lines derived from regression analysis of model test data takes the form:

$$C_P = k_c F r_p^{-b} \quad (4)$$

where k_c , b and n in Equation (3) are constants dependent on hull shape and friction coefficient. These relationships are valid across a wide range of hull shapes and friction coefficients, according to Colbourne (2000). The mean curve shapes are similar, but the magnitude and slope vary according to the hull shape and friction coefficient. In this study, it is assumed that the ship hull form can be divided into two categories, slender hull for container ships, and blunt hull for tankers, bulk carriers and general cargo ships. The prediction constants are derived from the model test data conducted by Guo et al. (2018) for a container ship, and Woolgar and Colbourne (2010) for a tanker, respectively. The values of these constants are presented in Table 1.

The ice resistance model used in this study is based on Equations (2)–(4), assuming the constants listed in Table 1 are applicable for the two case study vessels that will be presented in the later sections of this article. This is however a simplification because these constants were derived from model tests at relative lower speeds, which may introduce rather large uncertainties in resistance prediction. A more accurate ice resistance estimation requires additional model tests. Alternatively, high-fidelity computational models based on computational fluid dynamics (CFD), discrete element method (DEM), or finite element method (FEM) can be employed to better quantify ice-related resistances for individual ships. The authors are working on the numerical computation methods, aiming at improving the accuracy of the ice resistance

prediction. Nevertheless, despite of potential rather large errors in the predicted ice resistance values, the VPT searches for the optimal route with the lowest resistance, which is in line with the aim of voyage planning.

4. Ice-induced risk index outcome

Safe navigation in ice-infested waters depends on the severity of ice conditions, the ship's ice class, and the ship speed. Along with the Polar Code, IMO adopted the Polar Operational Limit Assessment Risk Indexing System (POLARIS), as a guidance on methodologies for assessing operational capabilities and limitations in ice (TraFi 2010). In contrast to the Polar Code, POLARIS is not mandatory, but could be included in some decision-support tools. In this study, POLARIS is implemented in the voyage planning tool. POLARIS calculates the risk index based on the following factors: the ship's ice class, the sea ice thickness (SIT), and the sea ice concentration (SIC)

Within POLARIS, the ship's ice class category is a combination of IACS Polar Class with FSICR. There are in total 12 ice classes: PC1 – PC7 plus IAS, IA, IB, IC and II classes. Each type of sea ice is associated with a certain ice thickness, with the hypothesis that ice age and thickness are generally well-correlated for a given time of year. A specific risk index value (RIV) in the range of 3 to -8 is assigned to each combination of ship ice class and ice thickness. Table 2 illustrates the RIVs for decayed ice conditions. The decayed ice condition is applicable in the summer Arctic, assuming sea ice decays in warm temperatures (TraFi 2010). For all ice classes, RIV = 3 should be used for ice-free conditions.

POLARIS uses a Risk Index Outcome (RIO) value to assess the limitation for operation in ice. For a specific ship and for each ice regime encountered, the RIVs are used to determine a RIO that forms the basis of the decision to operate or the limitation of the operations. The RIO is determined by a summation of the RIVs for each ice type present in the ice regime, multiplied by its partial concentration expressed in tenths:

$$\text{RIO} = (C_1 \times \text{RIV}_1) + (C_2 \times \text{RIV}_2) + \dots + (C_n \times \text{RIV}_n) \quad (5)$$

where $C_1 \dots C_n$ are the partial concentrations of the ice types within the ice regime, and $\text{RIV}_1 \dots \text{RIV}_n$ are the corresponding RIVs for each ice type. For sea ice in the Canadian Arctic region, partial concentrations can be obtained from ice charts

Table 2. Risk Index Values – decayed ice conditions.

	New ice	Gray ice	Gray white ice	Thin FYI 1st stage	Thin FYI 2 nd stage	Medium FYI 1st stage	Medium FYI 2nd stage	Thick FYI	Second Year ice	Light MYI	Heavy MYI
SIT in meter	[0, 0.1]	[0.1, 0.15]	[0.15, 0.3]	[0.3, 0.5]	[0.5, 0.7]	[0.7, 1.0]	[1.0, 1.2]	[1.2, 1.7]	[1.7, 2.0]	[2.0, 2.5]	>2.5
PC1	3	3	3	2	2	2	2	2	2	1	1
PC2	3	3	3	2	2	2	2	2	1	1	0
PC3	3	3	3	2	2	2	2	2	1	0	-1
PC4	3	3	3	2	2	2	2	1	0	-1	-2
PC5	3	3	3	2	2	2	2	1	-1	-2	-2
PC6	3	2	2	2	1	1	1	0	-2	-3	-3
PC7	2	2	2	1	1	1	0	-1	-3	-3	-3
IAS	2	2	2	2	1	1	0	-1	-3	-4	-4
IA	2	2	2	1	0	0	-1	-2	-4	-5	-5
IB	2	2	1	0	-1	-1	-2	-3	-5	-6	-6
IC	1	1	0	-1	-2	-2	-3	-4	-6	-7	-8
II	1	0	-1	-2	-3	-3	-4	-5	-7	-8	-8

provided by the National Ice and Snow Data Center or the Canada Ice Service. Similar open-access information on partial ice concentration is however unavailable for Russian Arctic sea ice. To calculate the RIO along the NSR, this study suggests a slightly different formula that only contains the ice concentration (SIC) and the RIV, which implies that the evaluated ice regime is assumed to be dominated by one homogenous ice type. The modified risk index outcome for the NSR is termed RIO*:

$$\text{RIO}^* = \text{RIV} \times \text{SIC} + 3 \times (10 - \text{SIC}) \quad (6)$$

The POLARIS standard addresses three levels of operational limitations: (i) normal operation; (ii) elevated operational risk; and (iii) operation subject to special consideration. For scenarios considered in the current study, the ship operations implemented in the VPT are based on the following criteria of RIO* values of each grid:

- $\text{RIO}^* > 0$: Normal navigation; the ship sails at a speed close to the service speed.
- $-10 < \text{RIO}^* \leq 0$: Elevated operational risk; the ship speed must be reduced depending vessel's ice class; Table 3 presents the recommended speed limits according to the POLARIS standard.
- $\text{RIO}^* \leq -10$: Operation subject to special consideration; the ship should not enter such ice regimes, and a different route must be taken.

5. Overview of the VPT

The voyage planning tool (VPT) presented in this study is an in-house MATLAB code. Figure 3 illustrates the flowchart of the VPT. Before running the VPT, the user needs to specify the ship type, the main dimensions as well as engine/propeller specifics. The ship performance model then automatically calculates the ship performance under various sea and operational conditions. Different ice resistance models can be implemented in the ship performance module. In this study, the ice resistance is computed from Equations (2)–(4) and added to the sum of the other resistance forces due to wave, wind, current, etc., resulting in the required thrust force as well as the fuel consumption. The output from the ship performance model is response surfaces that represent all combinations of environmental and operational conditions. A more detailed description of the VPT ship performance model can be found in Tillig (2017) and Tillig et al. (2017).

The routing module is based on Dijkstra's algorithm, a grid-based approach that aims to find the most cost-efficient path connecting any chosen nodes in a given grid (Dijkstra 1959). It needs to be highlighted that most of the algorithms are able to find out the optimal route which implies the choice of

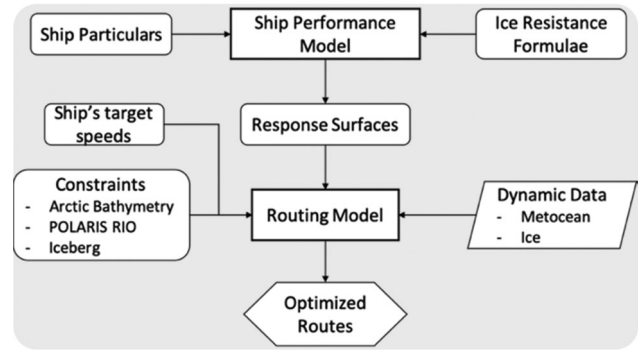


Figure 3. Flowchart of the VPT.

optimisation algorithm is unlikely to affect the outcome significantly. However, depending on the application regions, the computation time may differ considerably among different algorithms.

In the VPT, the constraint criteria from the POLARIS RIO as defined in Section 4 and the Arctic bathymetry are implemented in the routing module. The routing module reads in the response surfaces from the ship performance module, the ship target speeds specified by the user, and the ice and metocean data provided by the weather service agent. The routing module then automatically computes the most fuel-efficient path connecting those two points in that grid that can be arbitrary locations, which are treated as the start and endpoints of voyage. Detailed descriptions about the VPT routing module are referred to Rita (2018) and Li et al. (2019).

5.1. Ice and metocean data

For the purpose of voyage planning, ice and weather forecast data are required as inputs to the ship performance model. To accurately predict ship performance under various environmental loads in open and icy waters, the following data are needed:

- Wind: speed v_{wd} and direction θ_{wd} .
- Wave: significant wave height H_s and wave direction θ_{wd} .
- Ocean current: speed v_{oc} and direction θ_{oc} .
- Sea water: sea surface height H and sea surface temperature T .
- Ice: thickness (SIT) and concentration (SIC).

The above data are provided by the UK Met Office (www.metoffice.gov.uk), either directly via file transfer protocol (FTP) or disseminated through the Copernicus Marine Environment Monitoring Service (CMEMS). These datasets have been generated from the global UK Met Office models, which provide large-scale weather, ocean and sea ice short-range forecasts up to a week ahead. For the ice, meteorological and oceanographic data, nine regions have been cut-out to cover the operational voyage planning regions, over the periods July–October 2018 and July–October 2019. Figure 4 illustrates the spatial definitions of these regions. Among the nine regions, ice data are available in the Arctic, i.e. Murmansk to Bering Strait, the blue square in Figure 4.

Table 3. Recommended speed limit.

Ice Class	Recommended speed limit [knot]
PC1	11
PC2	8
PC3 – PC5	5
Below PC5	3

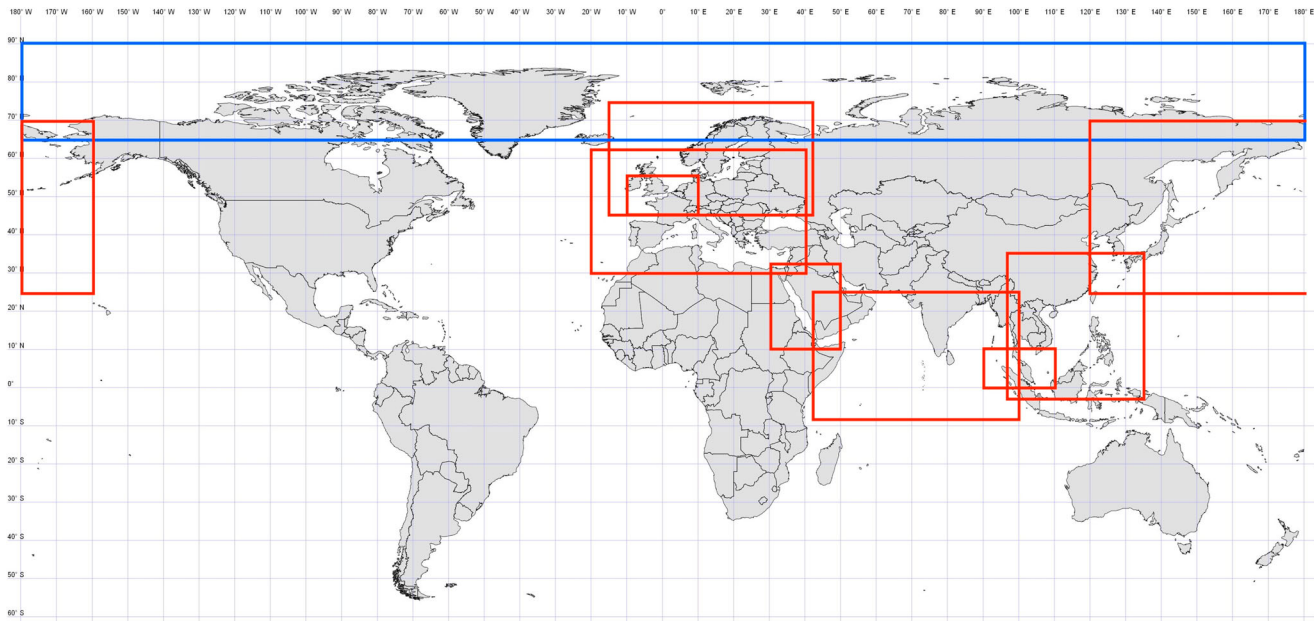


Figure 4. The voyage planning operational regions where ice, meteorological and oceanographic data are available. (This figure is available in colour online.)

- Europe – Murmansk: latitude $[45,75]^{\circ}\text{N}$; longitude $[-15,43]^{\circ}\text{E}$
- English Channel: latitude $[45,55]^{\circ}\text{N}$; longitude $[-10,10]^{\circ}\text{E}$
- Europe – Suez: latitude $[30,62]^{\circ}\text{N}$; longitude $[-20,40]^{\circ}\text{E}$
- Suez – Indian Ocean: latitude $[10,32]^{\circ}\text{N}$; longitude $[30,50]^{\circ}\text{E}$
- Indian Ocean – Strait of Malacca: latitude $[-8,25]^{\circ}\text{N}$; longitude $[41,100]^{\circ}\text{E}$
- Strait of Malacca: latitude $[0,10]^{\circ}\text{N}$; longitude $[90,110]^{\circ}\text{E}$
- Strait of Malacca – Shanghai: latitude $[-5,35]^{\circ}\text{N}$; longitude $[96,135]^{\circ}\text{E}$
- Bering Strait – Shanghai: latitude $[25,70]^{\circ}\text{N}$; longitude $[120,200]^{\circ}\text{E}$
- Murmansk – Bering Strait: latitude $[65,90]^{\circ}\text{N}$; longitude $[0,360]^{\circ}\text{E}$

5.2. Features of the VPT

The VPT in this study, compared with existing Arctic voyage planning programs, has the following advantages:

- The VPT aims at providing voyage planning support to cargo ships that are designed mainly for open water operations. It is therefore different from previous Arctic VPTs developed for icebreakers. The target scenarios are Arctic transits in the summer where the ice conditions differ significantly than those such as in winter Baltic.
- The VPT is not limited to voyage planning in the Arctic. Instead, the VPT is a ‘berth to berth’ solution, covering the entire sea routes between the origin and the destination ports in Europe and Asia. This implies the key environmental factors of wave, wind, and ice are all be treated in the VPT. For the ice-free Europe leg, i.e. from a European port to Novaya Zemlya, and the Asian Leg, i.e. from an Asian port to the Bering Strait, the VPT is also applicable,

providing functions similar to conventional weather routing tools for open water navigation.

- The optimisation objective of VPT is to minimise the fuel consumption of the entire voyage, which differs from many Arctic path planning tools that just aim to find out safe paths. In the VPT, safety is taken as a constraint, represented by the POLARIS criteria. The RIO* values used in the VPT is modified from the original one proposed by IMO, given the fact that forecasts of the partial ice concentration originally suggested by the Canadian Ice Service are simply unavailable along the NSR. In addition to the POLARIS constraint, the VPT plans the voyage considering the constraints of land, shallow water and potential icebergs.
- The proposed ice resistance model deals with fragmented ice floes that dominates in the Arctic waters in the summer. Both ice concentration and ice thickness are included when calculating the ice forces. This differs from most of ice routing tools that calculate ice resistance either in ridged ice fields or in brash ice channels opened by an icebreaker, for which the scenarios are frozen seas. For such types of ice, ice thickness is the only decisive factor in the ice resistance calculation.
- Another advantage of the VPT relies on the dynamic forecasts of ice, weather and sea conditions. These environmental forecast data with unified spatial resolutions are updated at least daily. During the voyage, newer routes will be continuously generated upon the updated forecasts, resulting in improved viability of the planned routes.

6. Case studies

Case studies using the VPT are presented for two vessels that plan to sail between Rotterdam and Shanghai. The voyages via the NSR are compared with the conventional routes via the Suez Canal, with respect to both the fuel consumptions and the total travel time. Vessel A is a general cargo ship that

Table 4. Characteristics of the case study ships.

Ship particulars	Vessel A	Vessel B
Ship type	General cargo	Container ship
Length overall (LOA) [m]	190	245
Breadth [m]	28.5	32.2
Draft [m]	11.0	10.8
Displacement [ton]	45,159	52,030
Design speed [knot]	14.8	21
Operational power [kW]	10,470	25,426
Operational propeller rpm [rpm]	124	93

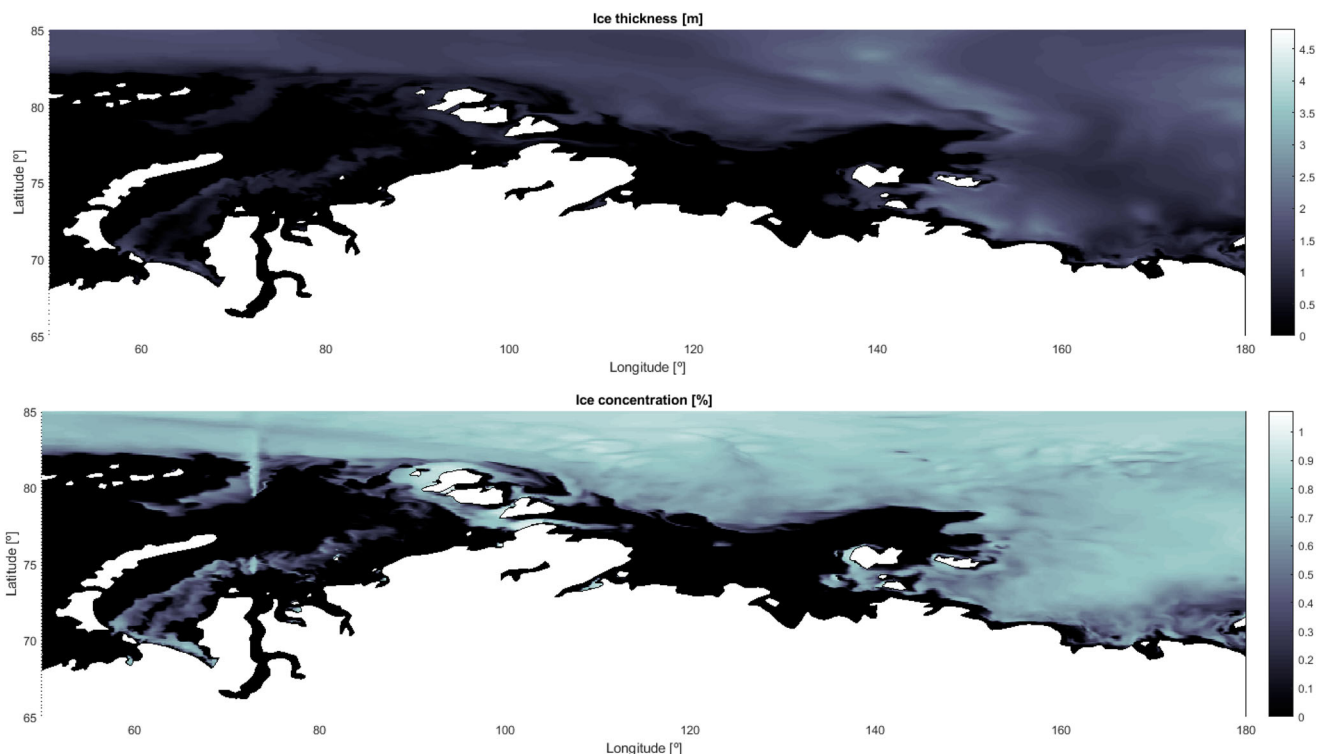
has been operating in the Arctic routes. Vessel B is a container ship that was selected to investigate the feasibility of container shipping via the NSR, with the consideration that the NSR is traditionally deemed to be more appealing to liquid, bulk and general cargo transportation (Zhang et al. 2016). Both vessels are of IA class according to FSICR, which is equivalent to IMO's PC6 class. The ship characteristics are presented in Table 4.

Although the VPT is supposed to receive frequently updated forecasts as input, in this demonstrating case, we employed historical metocean and ice data instead to demonstrate the functionality of the VPT. All the environmental variables were updated every 24 h. Iceberg position and motion are however unavailable in our data source. The function of iceberg avoidance is thus not activated in this case studies. Figure 5 illustrates the ice concentration and ice thickness in part of the NSR waters on July 15th, 2018. The ice data were obtained from the Copernicus Marine Environment Monitoring Service (CMEMS) as presented in Section 5.1.

Vessel A departed from Port Rotterdam on 1st July 2018, heading north and sailed along the North Sea, the Barents Sea, the NSR seas, the Bering Strait, and the North Pacific.

The target speed followed the real-life operational practice of this vessel and was set to 14.8 knots, except for in the Arctic waters between the Long Strait and the Vilkitsky Strait. This region covers the interior seas along the NSR such as the Laptev Sea and the East Siberian Sea, which receive significant ice floes transported from the central Arctic Ocean, including MYI as mentioned in Section 2.1. The target speed in this region is thus voluntarily reduced to 10 knots, following the practice of experienced Arctic ship masters (COSCO 2017). If severe ice conditions are encountered, the ship speed will be further reduced following the POLARIS ice operational limits as presented in Section 4: the ship sails at normal speed if the RIO* values are positive; upon elevated operational risk due to heavy ice, i.e. RIO* values are negative, the ship speed will be voluntarily reduced to 3 knots, which is recommended for IA class. The attained speeds in ice-infested water might be lower than the target speed. This involuntary speed reduction depends on both the ice conditions and the ship's power.

The total distance of the NSR voyage is 7752 nautical miles, taking 25.9 days, and consuming 531 tons of fuel. For the SCR voyage, Vessel A departed at the same time and place, but headed south instead. She took the route of the Mediterranean, the Suez Canal, the Indian Ocean, the Malacca Strait, and the South China Sea. The total distance is 10,054 nautical miles, taking 28.3 days, and consuming 761 tons of fuel. The total distances of the NSR and SCR of this case study are reasonably close to those found in the literature, 7869 nm for the NSR and 10,450 nm for the SCR (Zhang et al. 2016). It confirms that the NSR, for this specific case, saves distance, time and fuel. Figure 6 illustrates the two global routes of Vessel A. The case study results are summarised in Table 5.

**Figure 5.** Example ice data along the NSR; (above) ice thickness; (below) ice concentration. (This figure is available in colour online.)

A similar case study was carried out for Vessel B. The target speed of Vessel B was set to 21 knots. Like Vessel A, in the Arctic waters between the Long Strait and the Vilkitsky Strait, the target speed is reduced to 10 knots. In ice-infested waters, the same POLARIS ice operational limits were followed, i.e. when the ice conditions were deemed high, the speed was voluntarily reduced to 3 knots. The total distances, voyage periods and fuel consumptions for the NSR and the SCR routes are presented in Table 5 together with those of Vessel A. It is found that for the container ship, the NSR is not a time-saving option, despite of the shorter voyage distance. This is due to the speed reductions in Arctic waters. Nevertheless, the fuel saving potential when taking the NSR is observed, even though the exact fuel saving numbers need to be calibrated against measurements.

In the analysis of the results from the VPT, it is shown that when the ships were navigating in ice-infested waters, the VPT can search and suggest routes that least ice is encountered. Figure 7 shows an example of a route in the Kara Sea. The route deviates from the great circle route that is the shortest in distance. Instead, the route is optimised to avoid as much ice as possible. Figure 7 also shows that the routing algorithm not only accounts for the ice thickness but also the ice concentration. This indicates that the ice resistance model described in Section 3 is properly implemented in this voyage planning tool.

As stated previously, the VPT is not limited to route planning in the Arctic. In addition to ice, environmental factors such as wave, wind and current are also treated in the computation of ship performance, making the VPT a useful weather routing tool for open water conditions. Figure 8 illustrates the planned route in the Indian Ocean. The legend indicates the weight of wave; brighter means a higher wave. It is seen that the route was selected to avoid the high sea states that block the shortest route. The dynamic voyage planning function upon updated weather forecasts is deemed particularly useful for weather routing in areas like the Indian Ocean where storms are often encountered.

7. Uncertainties and future work

Rather large uncertainties are expected in the predicted fuel consumption numbers in the Arctic. The uncertainties come

Table 5. Comparison of the results of the NSR and SCR simulations.

Voyage data	Vessel A			Vessel B		
	NSR	SCR	Savings	NSR	SCR	Savings
Total distance [nm]	7752	10,054	22.9%	7861	10,099	22.3%
Total time [day]	25.9	28.3	8.5%	22.4	20.1	−11.6%
Fuel consumption [ton]	531	761	30.2%	1098	1608	32.9%

mainly from two sources: (1) the forecasts; and (2) the ice resistance model. Firstly, in comparison with open waters, forecasts of metocean and ice in Arctic seas are less validated by observation data, simply due to the remoteness in the Arctic. This implies the ice and weather inputs of the VPT might be less accurate as those in open waters. Secondly, the prediction constants in Table 3 are derived from model tests of lower relative speeds between ships and ice, which is expected to introduce uncertainties predicted resistance, and thereby the fuel consumption. This implies although the VPT finds the optimal routes, the predicted fuel consumption numbers need to be calibrated against measurement results.

In addition, all the cases presented in this study are independent operations, i.e. no icebreaker assistance has been included in the voyage planning models. In practice, however, many Arctic transits of low-ice-class ships were carried out with icebreaker escort or icebreaker convoy. Under icebreaker assistance, the voluntary speed reductions as required by the POLARIS ice operational limits become unnecessary, resulting in significantly shorter transit time than the above-mentioned independent operations. On the other hand, icebreaker assistance will add extra costs, which should also be considered in planning Arctic routes. The authors intend to include the options of icebreaker assistance in the VPT, taking different alternatives with regards to fuel and time savings, as well as the related costs into account.

8. Conclusions

The Arctic is rapidly transforming into a navigable ocean because of global warming. Shipping companies want to take the trans-Arctic routes to save time and costs and they need a reliable voyage planning tool. In this study, such a tool, the VPT, was presented. The VPT aims for improving fuel

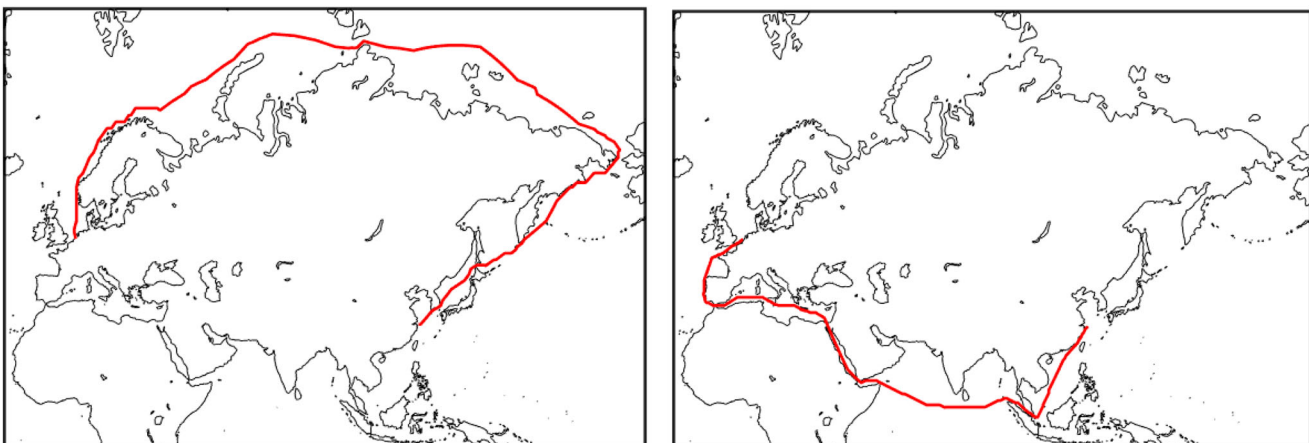


Figure 6. The Vessel A case study routes between Europe and Asia: the NSR route (left); and the route via the Suez Canal (right). (This figure is available in colour online.)

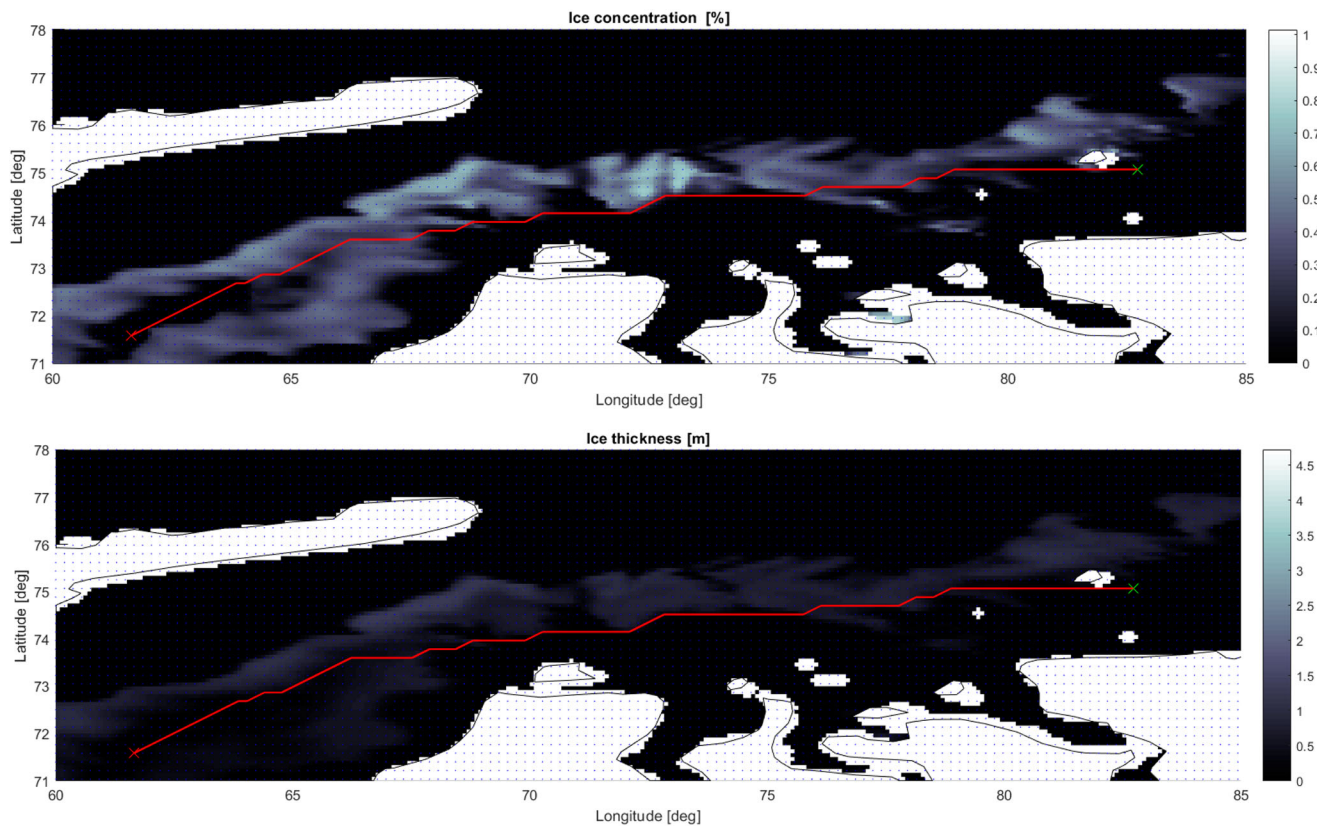


Figure 7. An example of a planned route in the Arctic against the ice concentration (upper) and the ice thickness (lower). (This figure is available in colour online.)

efficiency of existing and future cargo vessels that are designed mainly for open water operations. The VPT can take ice, wave, current, wind, water depth and temperature into consideration, making it a tool applicable not only for the Arctic but also for the open ocean. Characteristic Arctic ice conditions in the summer season are analyzed, which serves as the basis of the Arctic voyage planning. A modified POLARIS risk index outcome is adopted to evaluate the risk associated with ice voyage planning and serves as one of the major constraints in the VPT. The ice resistance model accounts for not only the ice thickness but also

the ice concentration of unconsolidated ice, while there remain uncertainties in the ice resistance model which will be addressed by future work using model tests and numerical simulations.

Case studies based on the summer Arctic transit scenarios have been carried out using the VPT. Two vessels, a general cargo ship and a container ship were selected as the case study vessels. Both the NSR and the traditional southern route via the Suez Canal were investigated. It is proved that the VPT finds the optimal routes with respect to fuel

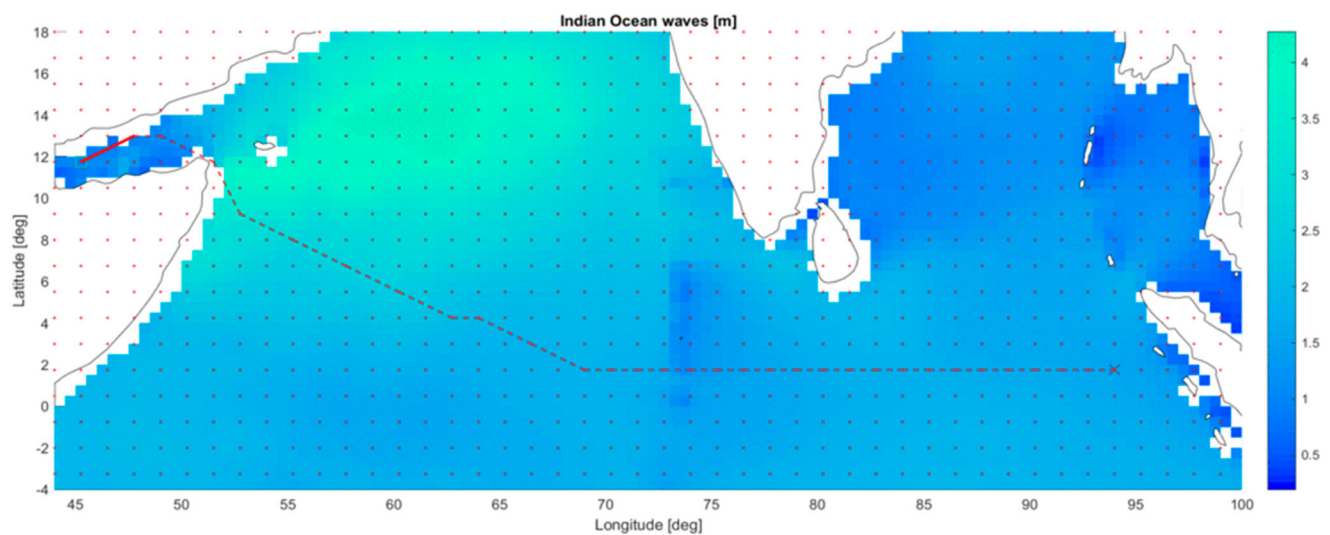


Figure 8. An example planned route in the Indian Ocean; the legend indicates the weight of wave. (This figure is available in colour online.)

consumption. For the general cargo ship, a large percentage of the sailing time is also found, which confirms previous studies. For the container ship, however, a saving of sailing time is unlikely for this specific case, which can be explained by the voluntary speed reductions in the Arctic waters. For both vessels, the fuel saving potential when taking the NSR is seen. Those results show potentials to apply the VPT to Arctic shipping.

Acknowledgements

The authors would like to thank Fabian Tillig at the Division of Marine Technology, Chalmers University of Technology for sharing his generic ship performance model.

Disclosure statement

No potential conflict of interest was reported by the authors.

Funding

This project received funding from the European Union's Horizon 2020 Research and Innovation Programme under Grant Agreement number: 723526, the SEDNA project.

ORCID

Zhiyuan Li  <http://orcid.org/0000-0001-6478-1027>

Jonas W. Ringsberg  <http://orcid.org/0000-0001-6950-1864>

References

- Balmasov S. 2018. Detailed analysis of ship traffic on the NSR in 2017 based on AIS data. [accessed 2018 Apr 17], Arctic Shipping Forum.
- Choi M, Chung H, Yamaguchi H, Nagakawa K. 2015. Arctic sea route path planning based on an uncertain ice prediction model. *Cold Reg Sci Technol.* 109(1):61–69.
- Choi KS, Nam JH, Park YJ, Ha JS, Jeong S-Y. 2010. Northern Sea Route transit analysis for large cargo vessels. Proceedings of the International Conference and Exhibition on Performance of Ships and Offshore Structures in Ice, Sep 20–23; Anchorage, Alaska, USA. Paper no. ICETECH10-173-RF.
- Colbourne D. 2000. Scaling pack ice and iceberg loads on moored ship shapes. *Ocean Eng Int.* 4(1):39–45.
- COSCO. 2017. China COSCO Shipping Corporation Limited. Internal Report no. 2017-X191.
- Dijkstra EW. 1959. A note on two problems in connexion with graphs. *Numer Math.* 1(1):269–271.
- Enkvist E. 1972. On the ice resistance encountered by ships operating in the continuous mode of icebreaking. *Swedish Academy of Engineering Sciences in Finland.* pp. 181.
- Guo CY, Xie C, Zhang JZ, Wang S, Zhao DG. 2018. Experimental investigation of the resistance performance and heave and pitch motions of ice-going container ship under pack ice conditions. *China Ocean Eng.* 32(2):169–178.
- Jeong SY, Kang KJ, Kim HS, Kim JJ, Roh MI. 2018. A study of ship voyage planning in the Northern Sea Route. Proceedings of the 13th ISOPE Pacific/Asia Offshore Mechanics Symposium, Oct 14–17; Jeju, Korea. Paper no. ISOPE-P-18-124.
- Jones SJ. 2004. Ships in ice – a review. Proceedings of the 25th Symposium on Naval Hydrodynamics, Aug 8–13; St. John's, Newfoundland and Labrador, Canada.
- Juva M, Riska K. 2002. On the power requirement in the Finnish-Swedish ice class rules. Winter Navigation Research Board, Research Report 53. Helsinki University of Technology, Ship Laboratory, Helsinki, Finland. pp. 80.
- Khon VC, Mokhov II, Latif M, Semenov VA, Park W. 2010. Perspectives of Northern Sea Route and Northwest passage in the twenty-first century. *Clim Change.* 100(3):757–768.
- Kotovirta V, Jalonen R, Axell L, Riska K, Berglund R. 2009. A system for route optimization in ice-covered waters. *Cold Reg Sci Technol.* 55(1):52–62.
- Li Z, Ringsberg JW, Rita FA. 2019. A voyage planning tool for Arctic transit of cargo ships. Proceedings of the ASME 2019 38th International Conference on Ocean, Offshore and Arctic Engineering (OMAE 2019), Jun 9–14; Glasgow, Scotland. Paper no. OMAE2019-95128.
- Lindquist A. 1989. Straightforward method for calculation of ice resistance of ships. Proceedings of the 10th International Conference on Port and Ocean Engineering under Arctic Conditions (POAC'89), Jun 12–16; Luleå, Sweden.
- Nam JH, Park I, Lee HJ, Kwon MO, Choi K, Seo YK. 2013. Simulation of optimal Arctic routes using a numerical sea ice model based on an ice-coupled ocean circulation method. *Int J Nav Archit Ocean Eng.* 5(2):210–226.
- Østreng W. 2013. The natural and societal challenges of the Northern Sea Route: a reference work. Springer Science & Business Media.
- Østreng W, Eger KM, Fløistad B, Jørgensen-Dahl A, Lothe L, Mejlænder-Larsen M, Wergeland T. 2013. Shipping in Arctic waters: a comparison of the Northeast, Northwest and trans polar passages. Springer Science & Business Media.
- Pharand D. 2007. The Arctic waters and the Northwest Passage: a final revisit. *Ocean Dev Int Law.* 38(1–2):3–69.
- Riska K, Wilhelmson M, Englund K, Leiviskä T. 1998. Performance of merchant vessels in ice in the Baltic. Winter Navigation Research Board, Research Report 52, Finnish Maritime Administration, Helsinki, Finland. pp. 72.
- Rita FA. 2018. Voyage planning tool: the Arctic Case [MSc Thesis no. 2018/37]. Department of Mechanics and Maritime Sciences, Chalmers University of Technology, Gothenburg, Sweden.
- Spencer D, Jones SJ, Colbourne DB. 1992. A proposed standard method for conduct and analysis of ice resistance model tests. Institute for Marine Dynamics, National Research Council Canada, St. John's, Newfoundland and Labrador, Canada.
- Tillig F. 2017. Generic model for simulation of the energy performance of ships – from early design to operational conditions [Thesis for the Degree of Licentiate of Engineering (Report no. 2017:02)]. Department of Mechanics and Maritime Sciences, Chalmers University of Technology, Gothenburg, Sweden.
- Tillig F, Ringsberg JW, Mao W, Ramne B. 2017. A generic energy systems model for efficient ship design and operation. *Proc Inst Mech Eng M: J Eng Marit Environ.* 231(2):649–666.
- TraFi. 2010. Finnish-Swedish Ice Class Rules (FSICR). [accessed 2019 Oct 27]: <https://www.traficom.fi/en/transport/maritime/ice-classes-ships>.
- Woolgar RC, Colbourne DB. 2010. Effects of hull–ice friction coefficient on predictions of pack ice forces for moored offshore vessels. *Ocean Eng.* 37(2–3):296–303.
- Zhang Y, Meng Q, Zhang L. 2016. Is the Northern Sea Route attractive to shipping companies? Some insights from recent ship traffic data. *Mar Policy.* 73:53–60.
- Zhang M, Zhang D, Fu S, Yan X, Goncharov V. 2017. Safety distance modeling for ship escort operations in Arctic ice-covered waters. *Ocean Eng.* 146(1):202–216.
- Zhang M, Zhang D, Fu S, Zhang C. 2018. A method for planning Arctic sea routes under multi-constraint conditions. Proceedings of International Conference on Port and Ocean Engineering under Arctic Conditions, Jun 10–16; Busan, Korea.